

2013

## Loss of DOK2 induces carboplatin resistance in ovarian cancer via suppression of apoptosis

E. Lum

M. Vigliotti

N. Banerjee

N. Cutter

K. O. Wrzeszczynski

*See next page for additional authors*

Follow this and additional works at: <https://academicworks.medicine.hofstra.edu/publications>



Part of the [Neoplasms Commons](#), and the [Obstetrics and Gynecology Commons](#)

---

### Recommended Citation

Lum E, Vigliotti M, Banerjee N, Cutter N, Wrzeszczynski K, Khan S, Kamalakaran S, Levine D, Dimitrova N, Lucito R. Loss of DOK2 induces carboplatin resistance in ovarian cancer via suppression of apoptosis. . 2013 Jan 01; 130(2):Article 54 [ p.]. Available from: <https://academicworks.medicine.hofstra.edu/publications/54>. Free full text article.

This Article is brought to you for free and open access by Donald and Barbara Zucker School of Medicine Academic Works. It has been accepted for inclusion in Journal Articles by an authorized administrator of Donald and Barbara Zucker School of Medicine Academic Works. For more information, please contact [academicworks@hofstra.edu](mailto:academicworks@hofstra.edu).

---

**Authors**

E. Lum, M. Vigliotti, N. Banerjee, N. Cutter, K. O. Wrzeszczynski, S. Khan, S. Kamalakaran, D. A. Levine, N. Dimitrova, and R. Lucito



## Loss of *DOK2* induces carboplatin resistance in ovarian cancer via suppression of apoptosis



Elena Lum<sup>a</sup>, Michele Vigliotti<sup>a</sup>, Nilanjana Banerjee<sup>b</sup>, Noelle Cutter<sup>a</sup>, Kazimierz O. Wrzeszczynski<sup>a</sup>, Sohail Khan<sup>c</sup>, Sitharthan Kamalakaran<sup>b</sup>, Douglas A. Levine<sup>d</sup>, Nevenka Dimitrova<sup>b</sup>, Robert Lucito<sup>e,\*</sup>

<sup>a</sup> Cold Spring Harbor, Woodbury, NY, United States

<sup>b</sup> Philips Inc., Briarcliff Manor, NY, United States

<sup>c</sup> Stony Brook University, Stony Brook, NY, United States

<sup>d</sup> Memorial Sloan Kettering Cancer Center, New York, NY, United States

<sup>e</sup> Hofstra North Shore-LIJ School of Medicine, Hempstead, NY, United States

### HIGHLIGHTS

- DNA methylation integrated with expression data in a panel of primary ovarian tumors identifies informatically significant genes correlated with platinum sensitivity.
- shRNA carboplatin resistance screen validates candidate genes functionally involved in resistance.
- *DOK2* downregulation induces carboplatin resistance via suppression of apoptosis/anoikis.

### ARTICLE INFO

#### Article history:

Received 22 December 2012

Available online 14 May 2013

#### Keywords:

Epigenetics  
Platinum resistance  
Genomics  
Ovarian Cancer  
Apoptosis

### ABSTRACT

**Objective.** Ovarian cancers are highly heterogeneous and while chemotherapy is the preferred treatment many patients are intrinsically resistant or quickly develop resistance. Furthermore, all tumors that recur ultimately become resistant. Recent evidence suggests that epigenetic deregulation may be a key factor in the onset and maintenance of chemoresistance. We set out to identify epigenetically silenced genes that affect chemoresistance.

**Methods.** The epigenomes of a total of 45 ovarian samples were analyzed to identify epigenetically altered genes that segregate with platinum response, and further filtered with expression data to identify genes that were suppressed. A tissue culture carboplatin resistance screen was utilized to functionally validate this set of candidate platinum resistance genes.

**Results.** Our screen correctly identified 19 genes that when suppressed altered the chemoresistance of the cells in culture. Of the genes identified in the screen we further characterized one gene, docking protein 2 (*DOK2*), an adapter protein downstream of tyrosine kinase, to determine if we could elucidate the mechanism by which it increased resistance. The loss of *DOK2* decreased the level of apoptosis in response to carboplatin. Furthermore, in cells with reduced *DOK2*, the level of anoikis was decreased.

**Conclusions.** We have developed a screening methodology that analyzes the epigenome and informatically identifies candidate genes followed by *in vitro* culture screening of the candidate genes. To validate our screening methodology we further characterized one candidate gene, *DOK2*, and showed that loss of *DOK2* induces chemotherapy resistance by decreasing the level of apoptosis in response to treatment.

© 2013 The Authors. Published by Elsevier Inc. Open access under [CC BY-NC-ND license](http://creativecommons.org/licenses/by-nc-nd/3.0/).

### Introduction

This year in the United States, more than 22,000 women will be diagnosed with ovarian cancer, and 15,500 will die of this disease.

Ovarian cancer is the leading cause of death from gynecologic cancer and the fifth most frequent cause of cancer-related death for women in the United States. Despite significant advances in surgical management and chemotherapy in the past few decades, the survival rate for ovarian cancer has not improved significantly. Presently the standard treatment is a platinum-based drug, such as carboplatin or cisplatin, combined with taxol. Unfortunately, approximately 25% of patients will present with primary platinum-resistant disease and will have very poor outcomes. Additionally, all patients whose tumors recur will ultimately develop acquired platinum resistance. At the heart of all cancers lies alterations at the genome level. These alterations, genetic

\* Corresponding author at: 500 Sunnyside Blv., Woodbury, NY, United States. Fax: +1 516 422 4109.

E-mail address: [robert.lucito@hofstra.edu](mailto:robert.lucito@hofstra.edu) (R. Lucito).

and epigenetic, alter gene function and play a role in the phenotype of the tumor, in some cases causing resistance to therapy. With recent analyses by our group and also by The Cancer Genome Atlas (TCGA) and others [1–3] many common genetic aberrations in ovarian carcinoma have been identified, but the mechanism of therapy resistance is poorly understood.

We have performed an epigenetic analysis of a set of primary ovarian cancer samples. Epigenetic modifications such as CG dinucleotide methylation can have far-reaching effects on cellular phenotypes, such as chemotherapy resistance. We have used an array-based methodology, Methylation Oligonucleotide Microarray Analysis (MOMA), to analyze 45 ovarian samples with 6 refractory samples, 9 resistant samples, 21 sensitive samples, and 9 normals. These data were then analyzed to identify genes that were differentially methylated between sensitive and resistant patients. Genes that were methylated and exhibited suppressed expression in platinum-resistant patients were identified. Since genes with acquired methylation in resistant patients could be candidates for resistance to carboplatin, we performed further function analysis of these genes. For these studies we developed a tissue culture platinum-resistance model. Three cell lines were selected with varying response to carboplatin, from sensitive to resistant. Thus far we have identified 19 genes in several different pathways that confer resistance to carboplatin.

One gene, *DOK2*, has been further characterized to demonstrate its ability to confer platinum resistance. We have shown that cells in which *DOK2* expression is suppressed are more resistant to platinum-based drugs, such as carboplatin. We have also shown that the increased resistance may be due to a change in the apoptotic response system. Interestingly *DOK2* is already known to be a tumor suppressor in lung cancer, and our studies demonstrate that loss of *DOK2* is tumorigenic, thus indicating tumor suppressor activity of *DOK2* in ovarian cancer cells, as well.

## Materials and Methods

### Cell Lines and Reagents

Cell lines included HOSE 6–3 (obtained from Dr. S. W. Tsao [4]); CAOV3 (ATCC# HTB-75); SKOV3 (ATCC# HTB-77); CAOV1 ovarian adenocarcinoma cell lines; and 293 T packaging cell line (ATCC# CRL-11268). MiR-30-lenti-based shRNA clones in a pGIPZ vector (clone ID V2LHS\_46643, V2LHS\_46640, and V3LHS\_367569), and Arrest-in transfection reagent were obtained from Open Biosystems. Retroviral shRNA clone in pSM2 vector (V2HS\_46640) subcloned into pMLP was obtained from Dr. L.V. Aelst. Virapower helper plasmid for lentiviral infection was obtained from Invitrogen. SYBR Green, reverse transcriptase and RNase inhibitor were purchased from Applied Biosystems. BSA was purchased through New England Biolabs and Bradford dye from Bio-Rad. Western blocking buffer was ordered from Sigma. Caspase 3,  $\gamma$ H2AX, and  $\beta$ -tubulin antibodies were obtained from Cell Signaling. Transwell assays and reagents were obtained from BD Bioscience. Carboplatin was purchased from Sigma. Radioactive carboplatin was supplied by Accelerated Medical Diagnostics. Primers were supplied by Sigma Genosys. NimbleGen photoprint arrays and MTT assays were supplied by Roche. Design of the array was described previously [5]. Datasets are available for methylation (Data Series GSE27940 — <http://www.ncbi.nlm.nih.gov/geo/query/acc.cgi?acc=GSE27940>) and expression (Affymetrix GSE27943 - <http://www.ncbi.nlm.nih.gov/geo/query/acc.cgi?acc=GSE27943>) data are available from Gene Expression Omnibus.

### Samples

Tumor DNA from 36 patients with advanced ovarian carcinomas treated at the Memorial Sloan Kettering Cancer Center during the period May 1992–February 2003 were included in this study. The

samples were collected under an informed consent and IRB approval [6]. Nine ovarian normal samples were obtained from The Cooperative Human Tissue Network, a repository of tumor material run by the National Institutes of Health.

### Chemotherapy Sensitivity and Survival

The ovarian cell lines HOSE, SKOV-3, CAOV3 and CAOV1 were tested for IC20, IC50 and IC80 carboplatin sensitivity levels. Each cell line was seeded at  $10^3$  cells/well in a 96 well plate and treated with carboplatin at a concentration range of 1–100  $\mu$ g/ml in 100  $\mu$ l of fully supplemented DMEM. After a period of 72 h proliferation was assessed by MTT 3-(4,5-dimethylthiazol-2-yl)-2,5-diphenyl tetrazolium bromide assay and absorbance measured at 595 nm using the Wallac microplate reader (Perkin Elmer).

### shRNA Screen

For each candidate gene, up to three miR30 shRNA clones in pLKO.1 and pGIPZ lentivirus vectors were selected from Open Biosystems Inc., propagated in bacteria and purified.

DNA from the virus pools were transfected into 293 T lentiviral packaging cell lines using Arrest-in and Virapower helper plasmid. A pool of GFP tagged pGIPZ empty vector was used to monitor transfection efficiencies. Efficiency of less than 70% was restarted (Fig. S1). Lentiviral supernatants were harvested 48–72 h post-transfection for infection of host cells. Cells were puro (2.5  $\mu$ g/ml) selected followed by carboplatin selection at the appropriate IC50 levels as previously determined (Fig. S2) for a total of 3 cycles of 3 days on carboplatin, 3 days off (onward, referred to as 3 cycle selection). Cells were harvested, genomic DNA isolated and the population of clones amplified and sequenced for identity.

### Viability Assay

Two sets of HOSE parental cell lines and HOSE shRNA *DOK2* cell lines were plated at  $5 \times 10^4$  cells/well in a volume of 500  $\mu$ l of medium per well in a 24-well plate in triplicate. The next day, one set of HOSE and HOSE shRNA *DOK2* was treated with carboplatin at the IC20, IC50, and IC80 concentrations and the other set (without carboplatin) was used as a control. After 3 days, cells were trypsinized and mixed in a 1:1 ratio with 0.4% trypan blue stain. The mixture was allowed to stand for 2–3 min. Viable cells with no blue stain and dead cells with blue stain were counted using a hemocytometer.

### Anoikis Assay

Cell suspensions were plated at  $1 \times 10^4$  cells/well at 100  $\mu$ l per well in a specialized 96-well anchorage resistant plate. Cells were treated with carboplatin at the IC20, IC50, and IC80 concentration and incubated at 37 °C for 3 days. A non-carboplatin treated set was prepared as a control. 500X Calcein AM/EthD-1 stock was diluted to 100X with culture medium. 1  $\mu$ l of the 100 $\times$  working stock of Calcein AM/EthD-1 was added to each well and incubated at 37 °C for 30–60 min. The cells were quantitatively measured using a fluorescent microplate reader at Ex: 485 nm and Em: 515 nm to measure viable cells with Calcein AM or at Ex: 525 nm and Em: 590 nm to detect dead cells with EthD-1.

### Immunoblotting

Protein lysates were extracted from HOSE and HOSE sh*DOK2* cell lines. A staurosporine treated HOSE cell line and UV control were used as control sets. Protein concentrations were determined using the Bradford Assay according to instructions, using BSA as standard to determine lysate concentrations. Western blots were performed

using 5–10  $\mu\text{g}$  of protein lysates according to standard procedures using the Invitrogen E-Page® system. After transfer of lysates from gel to PVDF membrane, blots were blocked and hybridized to Caspase 3 and  $\gamma\text{H2AX}$  anti-bodies diluted 1:1,000 overnight. Membranes were washed in TBS-Tween at room temperature. A fluorescently labeled anti-rabbit secondary antibody was diluted 1:10,000 and incubated for 30–60 min. Membranes were washed and protected from light. The odyssey infrared system was used to detect protein signals. Anti-rabbit monoclonal  $\beta$ -tubulin was used as a loading control.

#### Transwell Invasion Assay

A 24-well plate with transwell inserts coated with Matrigel was used as an invasion chamber. Cells were serum starved for a period of 16 h prior to the start of the invasion assay. Cell suspensions (500  $\mu\text{l}$ ;  $1 \times 10^5/\text{ml}$ ) in serum-free medium were added to the inserts. 750  $\mu\text{l}$  of DMEM with 15% FBS were placed in the lower wells as a chemoattractant and incubated for 24 h. Cells that had invaded to lower surface of the Matrigel-coated membrane were fixed with 4% methanol in PBS, stained with 1:1 dilution of crystal violet, and counted in five random fields using a brightfield microscope. The number of invading cells was quantified and normalized to mock-transfected controls.

## Results

#### Methylation Detection

For our methylation study, we selected 36 stage III or IV ovarian serous carcinoma samples that had accurate clinical annotation for platinum resistance, survival data for up to 10 years and also had associated expression data (Table S1). These samples were analyzed for methylation content using a previously developed method, Methylation Oligonucleotide Microarray Analysis (MOMA) [7], an array-based approach utilizing custom designed 380 K feature arrays that allowed tiling coverage of 26,219 out of 27,801 (HG17) annotated CpG islands. The association with the promoter was defined by the distance of any region of the island to the transcription start site. For this study we concerned ourselves mainly with promoter islands, whose genetic loci were within 2000 bp of the transcription start site. Geometric mean values are obtained for the CpG island probes of two dye-swap hybridizations from each sample.

#### Epigenetic Differences in Platinum Sensitivity

To identify genes involved in carboplatin resistance, we identified methylated regions that segregated with platinum sensitivity. We defined resistance according to the platinum free interval, the period between the last day of platinum treatment to the day of tumor recurrence. Patients tumors were grouped as refractory (tumors continued to grow or progress during treatment), resistance (tumors responded but recurred before 6 months), early sensitive (tumors recurred between 6 and 24 months), and late sensitive (tumors recurred after 24 months). We assayed 36 tumor and 9 normal samples with MOMA array technology. We removed the heterogeneous early sensitive group ( $n = 9$ ) from the chemoresistance analysis, leaving only the refractory/resistant samples ( $n = 15$ ) and late sensitive ( $n = 12$ ) patient categories.

To identify the probes that best differentiated resistant from sensitive samples, we performed Limma analysis using R/Bioconductor. Our rationale was that Limma analysis would be more adequate due to small number of available samples and very high number of microarray probes. Significance analysis was performed using the moderated t-statistic, which is computed for each probe between resistant and sensitive patient data ( $P < 0.05$ ). To increase stringency and identify a set of probes that would more accurately segregate tumors based

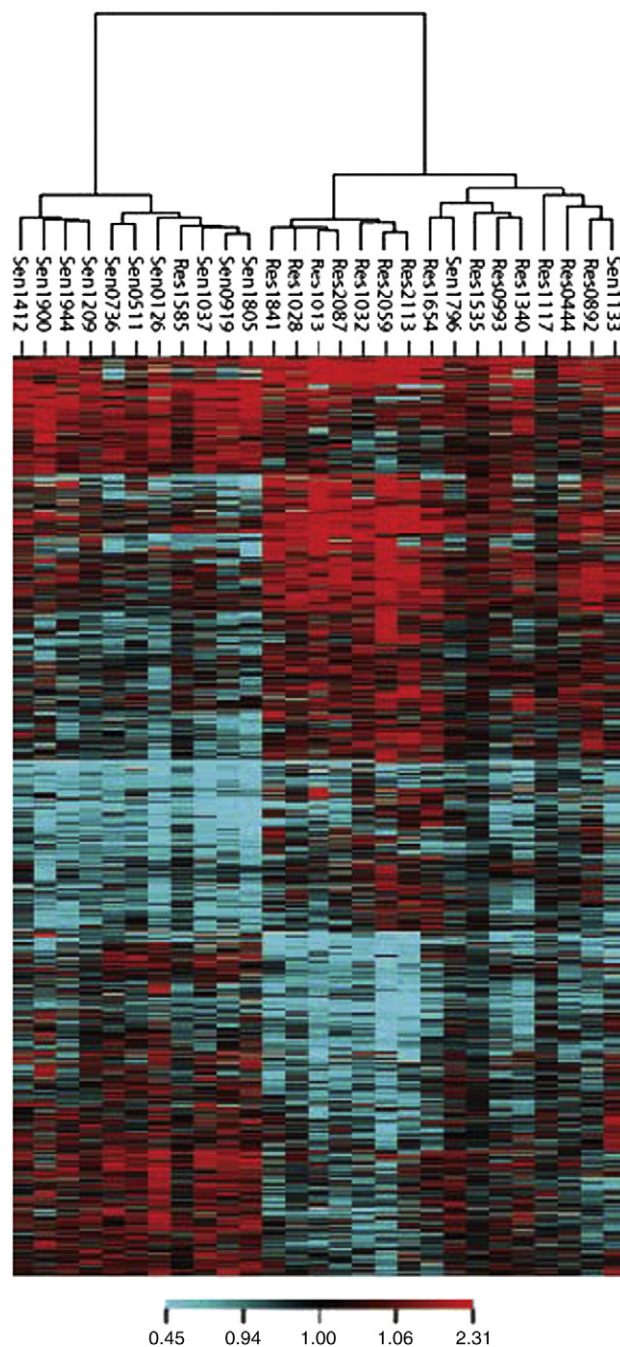


**Fig. 1.** Heatmap of the differentially methylated genes from the MOMA analysis showing segregation between the platinum therapy resistant and sensitive patient groups. This heatmap presents the results from the MOMA analysis. Hierarchical clustering was performed on the differentially methylated values from 749 probes that distinguished refractory/resistant and late sensitive patients. For these probes, hierarchical clustering using Pearson correlation as a distance metric was used. The distance metric is: 1- Pearson Correlation (x). The Ward method was utilized for finding clusters.

on carboplatin sensitivity, we performed a leave-one-out analysis ( $P < 0.05$ ). In each round, we left out a single sample and performed Limma test, and in the end kept only the probes that were statistically significant in all the 27 rounds when a single sample is left out. From this analysis we identified 749 probes whose methylation was significantly different between resistant and sensitive patients (Table S2). Fig. 1 presents the heatmap of the 749 differentially methylated probes showing the segregation of the resistant and sensitive patient groups. Since this analysis is based on the comparison of sensitive to resistant there are regions found more frequently methylated in resistant or



sensitive samples, breaking down to roughly 60% methylated in resistant and 40% methylated in sensitive tumors.

### Associating Methylation and Expression

For regions that differentiate between resistance and sensitivity, we next determined, which methylation event potentially represses transcription. For probes that were classified as being promoter CpG island probes, we performed in parallel differential methylation and differential expression analysis. Limma analysis and T-tests were done for each dataset to identify the most significant features (methylation probes or Affymetrix probe sets respectively) using a p-value of 0.05 as a cutoff. We then combined the methylation and expression datasets to determine which genes changed in methylation status with a corresponding expression change (whether increased or decreased). Of the original 749 probes that were statistically significant for methylation between resistant and sensitive patients, 509 were from promoters. After probes from the same gene were removed and remaining genes were matched to the Affymetrix U133A arrays used for the expression data, 296 significant genes were assessed for correlation between methylation and expression.

### In Vitro Platinum Screen

It was unclear if the gene candidates identified functionally altered platinum resistance in the cell. Thus we next tested the candidate genes in an *in vitro* carboplatin resistance assay. HOSE 6–3 (onward, will be referred to as HOSE), SKOV3, and CAOV3 cell lines were selected to perform functional studies. HOSE is a normal human ovarian surface epithelial cell line that has been immortalized by introduction of the HPV E6/7 ORF. This cell line has been previously used in the study of chemoresistance ([8–10]) and has been found to be very sensitive to carboplatin treatment. CAOV3 and SKOV3 are epithelial ovarian cancer cell lines and show a moderate to high resistance to carboplatin respectively.

We were most interested in genes that were methylated and transcriptionally repressed in platinum resistant patients. In total we identified approximately 296 gene candidates (Table S3). The suppression of transcription caused by methylation was modeled by the introduction of an shRNA clone. Since we had a large number of

candidates, we used a pooling strategy for the introduction of the shRNAs into the cells. By using 50 genes/pool (up to three shRNA clones per gene) 6 pools of shRNAs were assayed.

This first screen decreased the number of candidate genes by approximately 75%. To be more confident of the candidates, each shRNA clone was individually verified for carboplatin resistance using three concentrations of carboplatin, the IC20, the IC50, and the IC80. After the 3 cycle selection, we identified 19 positive hits (Table 1).

### Suppression of DOK2 Increases Platinum Resistance

Among the genes identified, to further validate our screening methodology, we selected *DOK2* for further functional characterization. *DOK2* has already been identified as a tumor suppressor in lung cancer ([11]) and its expression is suppressed in a number of other tumors ([12–15]). Cells infected with *DOK2* shRNAs were assayed by qPCR to ensure efficient knockdown of *DOK2* expression levels (Fig. S3). We went on to study the effect of *DOK2* suppression on carboplatin resistance using cells with shRNA suppression of *DOK2*.

*DOK2* suppression in cell lines resulted in a survival advantage with platinum treatment at the IC20, IC50, and IC80 with the 3 cycle selection protocol (Figs. 2 and S4). As it is a tumor suppressor, suppression of *DOK2* may increase carboplatin resistance by increasing cell growth and increasing the number of cells surviving treatment. To address this concern, growth assays were done over the course of 9 days without the addition of carboplatin, demonstrating that suppression of *DOK2* in HOSE, SKOV3, and CAOV1 cell lines had little effect on the number of cells growing (Fig. 3A–C). A 3-day Bromodeoxyuridine (BrdU) assay was also used to measure the level of actively dividing cells. Although the BrdU assay exhibited a slight selective growth advantage for *DOK2* knockdowns compared to their parental counterparts in the HOSE and SKOV3 cell lines, it was not statistically significant (Fig. 3D). We therefore concluded that increased resistance to carboplatin by suppression of *DOK2* is a result of some other mechanism other than increased growth of cells. It is important to note that although the CAOV3 cell line was used for the initial resistance screen, it was problematic for our functional studies because of a change in morphology after frequent passages. We therefore switched to a cell line exhibiting a similar level of sensitivity to carboplatin, CAOV1 (Fig. S2).

**Table 1**  
Single validation candidate genes.

Gene	Gene Description	Differential methylation p-value	Differential gene expression p-value	IC 20	IC 50	IC 80
GSK3B	Glycogen Synthase Kinase 3 Beta	0.011	N/A	+	+	+
DOK2	Docking Protein 2	0.013	N/A	+	+	+
APRT	Adenine Phosphoribosyltransferase	0.046	0.188	+	+	–
OXSRI	Oxidative-stress Responsive 1	0.024	0.808	+	+	–
CENPB	Major Centromere Autoantigen B	0.009	0.862	+	+	–
FZD1	Frizzled 1	0.015	0.508	+	+	+
ESRRA	Estrogen-related Receptor Alpha	0.022	0.464	+	–	–
HIRIP3	HIRA Interacting Protein 3	0.035	N/A	+	+	–
GTF2b	General Transcription Factor IIB	0.009	N/A	+	+	–
SGPL1	Sphingosine-1-phosphate Lyase 1	0.013	0.651	+	+	–
GABPA	GA Binding Protein Transcription Factor, Alpha	0.028	N/A	+	+	–
TWIST1	Transcription Factor	0.036	0.651	+	+	+
MDH1	Malate Dehydrogenase 1B, NAD (soluble)	0.038	0.277	+	+	+
NR2E1	Nuclear Receptor Subfamily 2, Group E, Member 1	0.053	N/A	+	+	–
NR3C2	Nuclear Receptor Subfamily 3, Group C, Member 2	0.017	N/A	+	+	–
SOX9	Transcription Factor	0.041	0.808	+	+	+
TOB1	Transducer of ERBB2, 1	0.017	N/A	+	+	+
UNG	Uracil-DNA Glycosylase Isoform UNG1 Precursor	0.012	0.277	+	+	–
ZIC1	Zinc Finger Protein of the Cerebellum 1	0.044	0.917	+	+	+

This table represents the genes that survived the pooled shRNA carboplatin screen at IC50. Each gene was singly validated with one shRNA clone per gene and underwent 3 cycle selection of platinum drugs at the IC20, IC50 and IC80 concentrations. Results of the single gene validation for each dose are presented along with differential methylation and differential expression p-values. Candidate genes for the pooled screen were selected based on significant p-values from the differential methylation data. Differential expression data is included for reference. For certain methylation probes, expression data was not available (N/A).

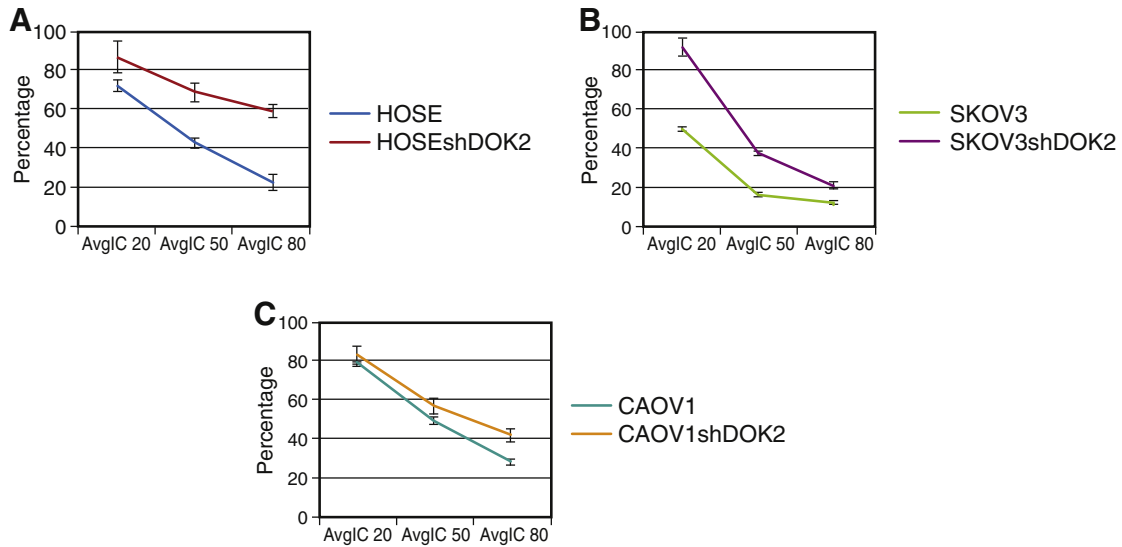


**Fig. 2.** Knockdown of *DOK2* increases platinum resistance in ovarian cell lines. Cell lines (A) HOSE (B) SKOV3 and (C) CAOV1 demonstrated suppression of *DOK2* with lentivirus increased resistance to carboplatin at the IC20, IC50, and IC80 concentrations after 9 days. Cells were plated at a density of  $1 \times 10^3$  cells/well in 96-well plates in triplicate. The IC concentrations on the x-axis is plotted against percentage survival on the y-axis. The results represent the mean  $\pm$  SD ( $n = 6$ ;  $P < 0.05$ ) in triplicate.

*Loss of DOK2 Protects Cells from Apoptosis and Anoikis*

An alternative role for *DOK2* in carboplatin resistance could be an effect on apoptosis. The deregulation of the apoptotic pathway is often shown to be involved in resistance [16–18], and this process can be derailed by epigenetic mechanisms [19]. To determine whether deregulating apoptosis is a mechanism of *DOK2*-mediated carboplatin resistance, we plated HOSE parental and HOSE shRNA *DOK2* cell lines with and without carboplatin. After 3 days, the percent viable cells to dead cells were determined using the crude and simple but very effective method of trypan blue stain exclusion from live cells. The results showed fewer dead cells in the shRNA *DOK2*

cell line compared to the parental HOSE cell line in the presence of carboplatin (Fig. 4A). To determine if any earlier marks of apoptosis such as levels of activated caspase 3 and  $\gamma$ H2AX phosphorylation, are affected by the loss of *DOK2*, western blots were performed to detect activated caspase 3 and  $\gamma$ H2AX phosphorylation after carboplatin treatment in cells with and without *DOK2*. We found decreased levels of activated caspase 3 and  $\gamma$ H2AX phosphorylation in cells with suppression of *DOK2* agreeing with our results from trypan blue exclusion (Fig. S5). Cells with *DOK2* suppression had less cell death and a subdued apoptotic response. These results suggest that aberrant apoptosis signals are a factor in how suppression of *DOK2* confers resistance to carboplatin.

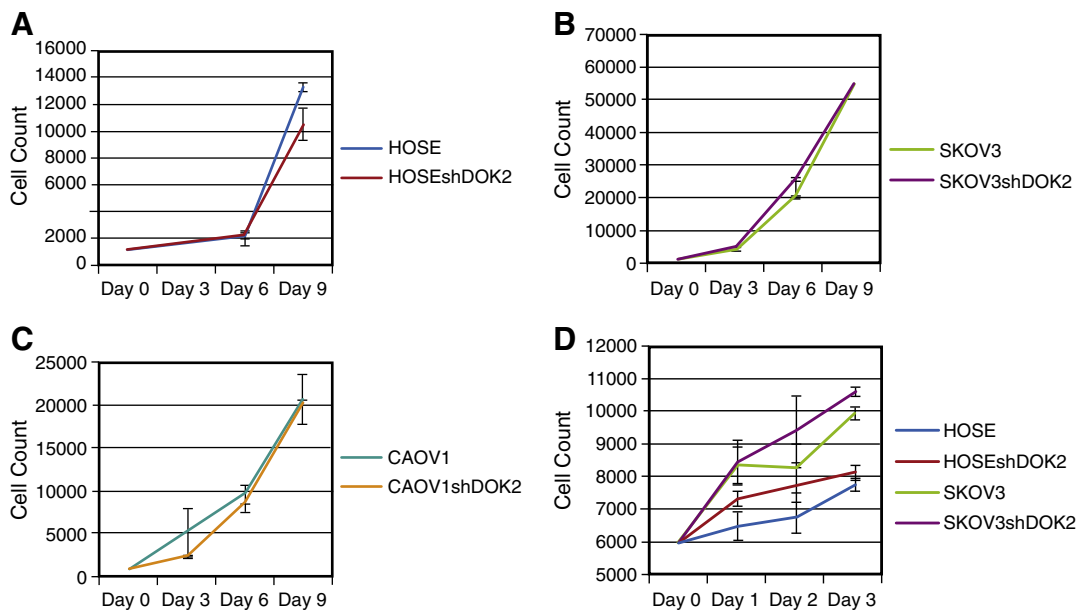


**Fig. 3.** *DOK2* silencing causes minimal effect on growth. A growth assay was also done over the course of 9 days showing that lentiviral *DOK2* shRNA infected ovarian cell lines, (A) HOSE, (B) SKOV3, and (C) CAOV1 causes little change in growth compared to their parental counterparts. Cells were plated at  $1 \times 10^3$  cells/well in 96-well plates in triplicate. The x-axis represents the time in days and the y-axis represents the cell count. The results represent the mean  $\pm$  SD ( $n = 6$ ;  $P < 0.05$ ) in triplicate. (D) 3-day BrdU assay to measure actively proliferating cells was done using HOSE and SKOV3 parental and lentiviral cell lines demonstrating a slight increase with *DOK2* suppression. Cells were plated at  $6 \times 10^3$  cells/well in 96-well plates in triplicate. The x-axis represents the time in days and the y-axis represents the cell count. The results represent the mean  $\pm$  SD ( $n = 4$ ;  $P < 0.05$ ) in triplicate.

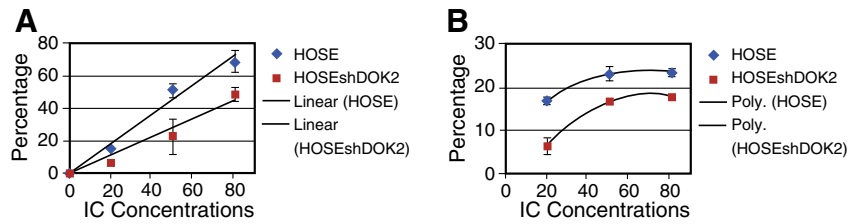


**Fig. 4.** *DOK2* silencing results in decreased apoptosis/anoikis induced cell death. (A) HOSE parental and HOSEsh*DOK2* were plated in triplicate on a 24 well plate at  $5 \times 10^4$  cells/well and treated with carboplatin at the IC20, IC50, and IC80. Live/dead cells were measured with trypan blue stain. The IC concentrations on the x-axis is plotted against percentage apoptotic on the y-axis. More dead cells were observed in the parental line in the presence of carboplatin. The results represent the mean  $\pm$  SD ( $n = 2$ ;  $P < 0.05$ ) in triplicate. (B) HOSE parental and HOSEsh*DOK2* were plated in triplicate on a 96-well low binding plate at  $1 \times 10^4$  cells/well and treated with carboplatin at the IC20, IC50, and IC80. Live cells were stained with the calcein AM and dead cells were stained with EthD-1 and the fluorescence signals were quantitatively measured using a fluorescence plate reader. The IC concentrations on the x-axis is plotted against percentage anoikis cells on the y-axis. A decrease in percentage of cell death was observed with loss of *DOK2*. The results represent the mean  $\pm$  SD ( $n = 2$ ;  $P < 0.05$ ) in triplicate.

Upon detachment of normal epithelial from the appropriate extracellular matrix, a specialized form of programmed cell death termed anoikis occurs to maintain tissue homeostasis and proper balance of cell differentiation [20,21]. However, anoikis resistance can interfere with this process and lead to the peritoneal dissemination of gastric and ovarian cancer cells [22]. We wanted to further explore whether the observed decreased cell death in the *DOK2* knockdown was due to protection from anoikis. We repeated the viability assay on low-binding tissue culture plates, using calcein AM dye to detect viable cells and ethium homodimer (EthD-1) to measure anoikis induced cell death. A noticeable difference was observed in the percentage of dead cells between parental and *DOK2* suppressed cells when examining for anoikis (Fig. 4B).

#### *DOK2* Silencing Confers an Invasive and Tumorigenic Phenotype In Vitro

In addition to its role in affecting apoptosis to confer carboplatin resistance, *DOK2* is also a known tumor suppressor in lung cancer [11]. However, its role in ovarian cancer has not been established. We therefore decided to explore whether *DOK2* displayed tumor suppressor features in ovarian cancer in culture. To measure tumorigenicity, we first assayed whether cell lines harboring the shRNA to *DOK2* required a basement membrane, and performed experiments for growth in soft agar [23,24]. *DOK2* shRNA lentiviral and retroviral cells were grown in soft agar for 3 weeks along with parental cell lines. *DOK2* suppression increased colony growth (Fig. S5). In addition, to measure invasive potential of the cells, a Matrigel assay was used to model the effects through a basement membrane. After 24 h there was a marked increase in the number of cells invading when *DOK2* was suppressed (Fig. 5). Scratch assays were also performed to evaluate migratory potential. Little migration was observed with parental cell lines while

increased migration was observed for cells with *DOK2* knockdown (Fig. S6). Our results suggest that in ovarian cancer cells, a decrease in the level of *DOK2* is associated with tumor suppressive features, such as increased invasiveness and tumorigenicity.

Since suppression of *DOK2* has tumor suppressive features in ovarian cell lines we next assessed if alteration of *DOK2* had an effect on clinical outcome by performing in silico analysis of public databases. We utilized the cBioPortal for Cancer Genomics (<http://www.cbioportal.org/public-portal/>) to determine first if *DOK2* alteration was found in patients ovarian tumors and if there was a significant difference in survival for these patients. Survival is a complex clinical variable affected by numerous parameters, gene alteration being only one of them. Using the whole tumor dataset there was no significant influence of *DOK2* alteration on survival but if the patients with a complete response to platinum treatment were selected (276 patients) *DOK2* alteration was significant in both overall survival (p-value of 0.031334) as well as disease free survival (p-value of 0.018653) (Fig. S8 Panels A and B respectively). Furthermore if only homozygous deletions were assessed for significant affect on survival the p-value was even stronger (0.001515 for overall survival and 0.000675 for disease free survival, data not shown) but only 4 samples had *DOK2* alteration. These data suggests alteration of *DOK2* has a significant effect on survival likely to be exerted by its effect on treatment response and/or tumor suppressive activity.

#### Discussion

Chemo-resistance in ovarian cancer, as in many other cancers, is an important clinical issue. The genome alterations that are responsible for a tumor's ability to resist treatment are often caused by genetic mutations or epigenetic alterations. While others have looked

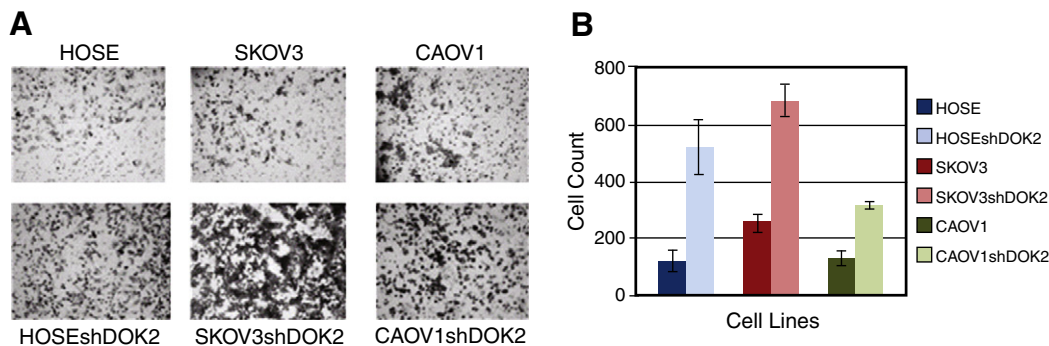


**Fig. 5.** Suppression of *DOK2* showed increased invasive potential. (A) The matrigel invasion assay was used to determine invasive potential. The upper chamber was plated with  $5 \times 10^4$  cells/ml of serum starved cell suspensions. The bottom chamber was filled with medium containing 15% FBS, used as a chemoattractant. After 24 h there was a marked increase of invading cells through the matrigel. (B) Quantification of cell count showed suppression of *DOK2* via lentivirus greatly increased number of invading cells, demonstrating increased invasive properties. Counts were based on an average cell count of 5 random areas viewed under  $40\times$  magnification. The cell count for each cell line is shown. The results represent the mean  $\pm$  SD ( $n = 6$ ;  $P < 0.05$ ) in triplicate.



at the genome of ovarian cancer to study outcome or therapy response, we have looked at the epigenome to determine whether genes suppressed by DNA methylation have a role in therapy resistance. We utilized a three step screening methodology to identify candidate genes that were involved in chemo-resistance. First, we used genome wide screening to identify epigenetic alterations that occur in ovarian tumors. Next, we used informatics and statistical methods to identify alterations that could segregate resistant from sensitive patients. Lastly, we utilized an *in vitro* cell culture shRNA screen to identify genes that when epigenetically suppressed increased platinum resistance.

The clustering of the epigenetic and informatics screening results segregated the samples along carboplatin resistance, based on Limma analysis, showing that among the 749 identified candidate probes there is a difference in methylation patterns between the resistant and sensitive patients. Since oncogenesis may not be a prerequisite to chemotherapy resistance, it was not surprising that we did not identify a large number of tumor suppressors and oncogenes (data not shown). A number of well-characterized genes were identified that have been linked to resistance, such as PTEN and HIF1 [25–28].

Our informatics screen defined a list of candidate genes that were assayed with our *in vitro* carboplatin shRNA tissue culture screen. Of the positive hits from the screening, there were a number of notable genes, including *SOX9*, *ZIC1*, *TWIST* (involved in EMT) [29–35], *GSK3B* and *FZD1* (both involved in WNT signaling) [36,37]. The screen successfully validated that some of the genes identified with epigenetic alterations could affect carboplatin sensitivity in the cells. To further validate the screen, we went on to characterize the cellular mechanism altered by the *DOK2* proteins that led to carboplatin resistance.

One major path of resistance involves deregulating apoptosis. Dysfunctional apoptotic responses may result in uncontrolled cell growth, leading to cancer [38]. The effectiveness of most chemotherapies, such as platinum therapy relies heavily on their ability to induce apoptosis. As a consequence, chemo-resistant cells often have down-regulated pro-apoptotic genes or up-regulated anti-apoptotic genes. In addition to key regulators in the apoptotic pathway, DNA methylation of gene targets has also been shown to affect various mechanisms of therapy, including membrane transport, drug metabolism, DNA repair, and apoptosis [19].

In ovarian cancer, intraperitoneal fluid accumulates resulting in a buildup of non-adherent cancerous ascites cells [39]. Tumor cells in ascites must bypass suspension-induced apoptosis, or anoikis, to spread to distant organs [22]. *DOK2*, in addition to decreasing the level of classical apoptosis, could also suppress the level of anoikis. We propose that suppression of *DOK2* gives ovarian tumor cells a selective advantage in becoming chemotherapy resistant non-adherent tumor cells in ascites. Suppression of anoikis has been reported to promote metastasis and resistance to chemotherapy in certain cancers, including breast and ovarian cancers [40].

The link between anoikis resistance with anchorage independency and metastasis [41] prompted us to test whether suppression of *DOK2*, in addition to suppressing anoikis, also increased a tumorigenic phenotype. Indeed the loss of *DOK2* induced a tumorigenic phenotype in ovarian cell lines. We propose that loss of contact inhibition and increased invasive properties observed in *DOK2* suppressed cells, while being typical hallmarks of cancer cells, are key components of anoikis suppression, as well.

Our lab has developed a chemo-resistance screen to identify what epigenetic changes occurred in primary ovarian tumor samples and has characterized which of these functionally alter carboplatin resistance. Recent evidence finding some serous ovarian cancers are likely to originate from fallopian tubes rather than ovarian epithelia raises questions for the analysis of *DOK2*. In the future, it will be useful to utilize both an immortalized ovarian and fallopian tube epithelial cell lines. However this recent data concerning the cell of origin for EOC does not affect the selection of genes for our screen, since all of our analysis

revolved around the comparison of tumor to tumor for both methylation and expression. One gene found methylated, *DOK2*, was selected and we demonstrated that suppression of this gene increases carboplatin resistance by decreasing both classical apoptosis and the non-adherent form of apoptosis, anoikis, a mechanism that is critical to ovarian cancers progression by ascites associated metastasis. We also show that suppression of *DOK2*, a known tumor suppressor in lung cancer, appears to have tumor suppressor features in ovarian cancer as well. These results validate our approach to finding genes epigenetically regulated that are involved in chemo-resistant ovarian cancer. We have made our results publicly available in the Gene Expression Omnibus database for the ovarian cancer community (see materials and methods). Understanding the molecular events that lead to chemotherapy resistance will allow us to develop more suitable chemotherapy regimens, learn how to re-sensitize cells to current drugs, and improve current drug designs or invent novel therapeutics.

Supplementary data to this article can be found online at <http://dx.doi.org/10.1016/j.ygyno.2013.05.002>.

#### Conflict of Interest Statement

The authors declare no conflicts of interest.

#### Acknowledgements

This work was supported by Philips Research, the Starr Foundation, Department of Defense [W81XWH-05-1-0068 to R.L.], and Chia Family Foundation [D.A.L.]. We also thank Linda Van Aelst, Ph.D for her generous donation of retroviral vector samples and Scott Powers, Ph.D for his guidance and helpful discussions.

#### References

- [1] Cancer Genome Atlas Research Network. Integrated genomic analyses of ovarian carcinoma. *Nature* 2011;474(7353):609–15.
- [2] Wang ZC, et al. Profiles of genomic instability in high-grade serous ovarian cancer predict treatment outcome. *Clin Cancer Res* 2012;18(20):5806–15.
- [3] Bast Jr RC, Hennessy B, Mills GB. The biology of ovarian cancer: new opportunities for translation. *Nat Rev Cancer* 2009;9(6):415–28.
- [4] Tsao SW, et al. Characterization of human ovarian surface epithelial cells immortalized by human papilloma viral oncogenes (HPV-E6E7 ORFs). *Exp Cell Res* 1995;218(2):499–507.
- [5] Lucito R, et al. Representational oligonucleotide microarray analysis: a high-resolution method to detect genome copy number variation. *Genome Res* 2003;13(10):2291–305.
- [6] Naume B, Zhao X, Synnestevedt M, Borgen E, Russnes HG, Lingjærde OC, et al. Presence of bone marrow micrometastasis is associated with different recurrence risk within molecular subtypes of breast cancer. *Mol Oncol* 2007;1(2):160–71.
- [7] Kamalakaran S, et al. Methylation detection oligonucleotide microarray analysis: a high-resolution method for detection of CpG island methylation. *Nucleic Acids Res* 2009;37(12):e89.
- [8] Siu MK, et al. Stem cell transcription factor NANOG controls cell migration and invasion via dysregulation of E-cadherin and FoxJ1 and contributes to adverse clinical outcome in ovarian cancers. *Oncogene* 2012 [in press].
- [9] Liao X, et al. Aberrant activation of hedgehog signaling pathway in ovarian cancers: effect on prognosis, cell invasion and differentiation. *Carcinogenesis* 2009;30(1):131–40.
- [10] Chan DW, et al. Loss of MKP3 mediated by oxidative stress enhances tumorigenicity and chemoresistance of ovarian cancer cells. *Carcinogenesis* 2008;29(9):1742–50.
- [11] Berger AH, et al. Identification of DOK genes as lung tumor suppressors. *Nat Genet* 2010;42(3):216–23.
- [12] Niki M, et al. Role of Dok-1 and Dok-2 in leukemia suppression. *J Exp Med* 2004;200(12):1689–95.
- [13] Yasuda T, et al. Role of Dok-1 and Dok-2 in myeloid homeostasis and suppression of leukemia. *J Exp Med* 2004;200(12):1681–7.
- [14] An CH, et al. Mutational and expression analysis of a haploinsufficient tumor suppressor gene *DOK2* in gastric and colorectal cancers. *APMIS* 2011;119(8):562–4.
- [15] Mashima R, et al. Mice lacking Dok-1, Dok-2, and Dok-3 succumb to aggressive histiocytic sarcoma. *Lab Invest* 2010;90(9):1357–64.
- [16] Fojo T. Cancer, DNA repair mechanisms, and resistance to chemotherapy. *J Natl Cancer Inst* 2001;93(19):1434–6.
- [17] Morrison T, et al. Targeting the mechanisms of resistance to chemotherapy and radiotherapy with the cancer stem cell hypothesis. *J Oncol* 2011;2011:941876.
- [18] Gottesman MM. Mechanisms of cancer drug resistance. *Annu Rev Med* 2002;53:615–27.
- [19] Balch C, et al. Role of epigenomics in ovarian and endometrial cancers. *Epigenomics* 2010;2(3):419–47.
- [20] Frisch SM, Sreaton RA. Anoikis mechanisms. *Curr Opin Cell Biol* 2001;13(5):555–62.

- [21] Zhan M, Zhao H, Han ZC. Signalling mechanisms of anoikis. *Histol Histopathol* 2004;19(3):973–83.
- [22] Kim YN, et al. Anoikis resistance: an essential prerequisite for tumor metastasis. *Int J Cell Biol* 2012;2012:306879.
- [23] Cifone MA, Fidler IJ. Correlation of patterns of anchorage-independent growth with in vivo behavior of cells from a murine fibrosarcoma. *Proc Natl Acad Sci U S A* 1980;77(2):1039–43.
- [24] Macpherson I, Montagnier L. Agar suspension culture for the selective assay of cells transformed by polyoma virus. *Virology* 1964;23:291–4.
- [25] Daponte A, et al. Prognostic significance of hypoxia-inducible factor 1 alpha (HIF-1 alpha) expression in serous ovarian cancer: an immunohistochemical study. *BMC Cancer* 2008;8:335.
- [26] Bachtary B, et al. Overexpression of hypoxia-inducible factor 1alpha indicates diminished response to radiotherapy and unfavorable prognosis in patients receiving radical radiotherapy for cervical cancer. *Clin Cancer Res* 2003;9(6):2234–40.
- [27] Enatsu S, et al. Expression of hypoxia-inducible factor-1 alpha and its prognostic significance in small-sized adenocarcinomas of the lung. *Eur J Cardiothorac Surg* 2006;29(6):891–5.
- [28] Sun HC, et al. Expression of hypoxia-inducible factor-1 alpha and associated proteins in pancreatic ductal adenocarcinoma and their impact on prognosis. *Int J Oncol* 2007;30(6):1359–67.
- [29] Wu JH, et al. Identification of DNA methylation of SOX9 in cervical cancer using methylated-CpG island recovery assay. *Oncol Rep* 2012 Jan;29(1):125–32.
- [30] Sun M, et al. SOX9 expression and its methylation status in gastric cancer. *Virchows Arch* 2012;460(3):271–9.
- [31] Gan L, et al. ZIC1 is downregulated through promoter hypermethylation, and functions as a tumor suppressor gene in colorectal cancer. *PLoS One* 2011;6(2):e16916.
- [32] Ezponda T, et al. The histone methyltransferase MMSET/WHSC1 activates TWIST1 to promote an epithelial-mesenchymal transition and invasive properties of prostate cancer. *Oncogene* 2012 [in press].
- [33] Xue G, et al. Akt/PKB-mediated phosphorylation of Twist1 promotes tumor metastasis via mediating cross-talk between PI3K/Akt and TGF-beta signaling axes. *Cancer Discov* 2012;2(3):248–59.
- [34] Giordano A, et al. Epithelial-mesenchymal transition and stem cell markers in patients with HER2-positive metastatic breast cancer. *Mol Cancer Ther* 2012 Nov;11(11):2526–34.
- [35] Gomez I, et al. TWIST1 is expressed in colorectal carcinomas and predicts patient survival. *PLoS One* 2011;6(3):e18023.
- [36] Katoh M. Cross-talk of WNT and FGF signaling pathways at GSK3beta to regulate beta-catenin and SNAIL signaling cascades. *Cancer Biol Ther* 2006;5(9):1059–64.
- [37] Malbon CC. Frizzleds: new members of the superfamily of G-protein-coupled receptors. *Front Biosci* 2004;9:1048–58.
- [38] Li J, et al. Human ovarian cancer and cisplatin resistance: possible role of inhibitor of apoptosis proteins. *Endocrinology* 2001;142(1):370–80.
- [39] Tang MK, et al. c-Met overexpression contributes to the acquired apoptotic resistance of nonadherent ovarian cancer cells through a cross talk mediated by phosphatidylinositol 3-kinase and extracellular signal-regulated kinase 1/2. *Neoplasia* 2010;12(2):128–38.
- [40] Simpson CD, Anyiwe K, Schimmer AD. Anoikis resistance and tumor metastasis. *Cancer Lett* 2008;272(2):177–85.
- [41] Guadamillas MC, Cerezo A, Del Pozo MA. Overcoming anoikis—pathways to anchorage-independent growth in cancer. *J Cell Sci* 2011;124(Pt 19):3189–97.
- [42] Bolstad BM, et al. A comparison of normalization methods for high density oligonucleotide array data based on variance and bias. *Bioinformatics* 2003;19(2):185–93.
- [43] Benjamini Y, Hochberg Y. Controlling the false discovery rate: a practical and powerful approach to multiple testing. *J R Stat Soc Ser B* 1995(57):289–300.
- [44] Pollard K, Dudoit S, van der Laan MJ. Multiple testing procedures: R multtest package and applications to genomics. *Berkeley Division of Biostatistics Working Paper Series*, 164; 2004 [U.C.].